Location Determination Methods Employing a Network of Passive Beacons[1,2]

Andrew Gray Clayton Okino Esther H. Jennings
Jet Propulsion Laboratory
California Institute of Technology
4800 Oak Grove Drive
Pasadena, CA 91109
(818)354-4906 (818)393-6668 (818)354-1390
{Andrew.Gray,cokino,estherj}@jpl.nasa.gov

Abstract- A mobile sensor platform that is capable of determining its precise location on the surface of Titan, or other extra-terrestrial area without a global positioning system (GPS) or orbiter, has tremendous science value. This capability can allow the in-situ sensor platform to remain at or even return to a location of high scientific interest with great precision, as well as to determine the precise position science data is collected. We present an overview of in-situ navigation architectures utilizing various methods for performing fast, precise, in situ location determination needed by an aerial vehicle acting as a mobile sensor platform on Titan, one of Saturn's moons, without the use of an orbiter. Emphasis is placed on architectures that utilize potentially low-cost passive beacons. The fine resolution navigation or in-situ location determination may be used in conjunction with "course" navigation obtained via a long haul link to Earth. The "course" navigation allows the aerial vehicle to move between networks of beacons that are deployed at locations of high science interest.

TABLE OF CONTENTS

1. INTRODUCTION

Current objectives of the science community studying Titan dictate the need for an in- situ science-gathering platform. This platform will most likely be an aerial vehicle or aerobot of some type. In addition, recent efforts to define lower cost Titan exploration architectures delete the orbiter, making the problem of location determination and navigation of the in situ vehicle even more difficult. The proposed aerial vehicles and the many possible variations share common problems without known feasible solutions. In particular we seek a solution for fast, precise, in situ location determination needed by the aerial vehicle on Titan.

A mobile science platform capable of determining its precise location on the surface of Titan has tremendous science value. This for instance will allow the platform to remain at or even return to a location of high scientific interest with great precision, as well as to determine the precise time and position science data is collected. These capabilities are extremely useful in studying evolutionary processes, erosion, and such things as cryo-volcanic activity. Furthermore, the ability to determine precise location enables the aerial vehicle to navigate a prescribed route without getting lost or inadvertently retracing previous routes. Finally, real-time or near real-time location determination appears to be a necessary tool for the aerial vehicle to meet science objectives in the time-varying and potentially unfavorable atmospheric conditions on Titan. The in situ navigation methods described in this paper provide "fine" relative navigation on short time scales (sub-second) and operate in conjunction with the "course" absolute navigation provided by long haul Earth-Titan navigation on much longer time scales (hours +).

The major challenge is to develop an architecture (navigation map) to provide location determination useful for the exploration vehicle navigation in the dynamic atmosphere of Titan. This architecture must take into consideration area of coverage, cost/mass/size and power limitation of beacons, RF propagation and dynamics of the atmosphere.

We identify the use of low cost methods that incorporate low cost/mass beacons to help solve the problems of location determination and navigation. Low cost/mass beacons, when deployed in the appropriate location determination architecture (navigation map) may be used by the aerial vehicle to establish its location on Titan in near real-time without an orbiter. These beacons could be deployed on the surface of Titan by the aerial vehicle in a

[1] 0-7803-7651-X/03/$17.00 © 2003 IEEE
[2] IEEEAC paper # 1353, Updated December 13, 2002

number of ways. Presumably, during a beacon deployment, the vehicle would transmit to Earth for the purpose of obtaining an absolute location estimate. Many such beacons, once deployed, would provide a navigation map that the aerial vehicle could use to determine relative location (relative to the fixed map of beacons) nearly instantaneously. In addition to the benefits to navigation and science already mentioned, the use of beacon technology may augment altimeter and accelerometer instrumentation used for science and aerial vehicle health (collision avoidance).

The navigation map design (e.g. beacon spacing) utilized by the aerial vehicle is primarily determined by the science objectives and parameters (many dynamic) of the system. In addition, the two general classes of beacons, passive and active beacons, used to implement the architecture will also greatly impact the design of the navigation map. Furthermore, any such navigation map design must consider the mission cost, size/mass/power and numerous limitations on technology imposed by the environment of Titan.

We leverage the use of a navigation map architecture composed of realizable surface beacons suitable for providing near-real time location determination for an aerial vehicle on Titan. The architecture will be designed with consideration of the following: estimates of aerial vehicle altitude and speed ranges, estimates of radio-frequency propagation characteristics, and science gathering methods.

Motivation of technology for Titan

Titan, Saturn's largest moon, has been identified as the only body in the solar system besides Earth with a significant nitrogen atmosphere and contains considerable amount of organic photochemistry[1]. Moreover, Titan's atmosphere contains hydrocarbon elements that are the building blocks for amino acids necessary for the formation of life.

In late 1970s and early 1980s, Pioneer and Voyager spacecraft flew by the Saturn system. Due to Titan's thick atmosphere, about four times as dense as Earth's atmosphere, the hydrocarbon haze was not penetrable to the cameras on board Pioneer or Voyager, and the close up pictures taken revealed only variations of brightness of the atmosphere and clouds. The Hubble Space Telescope has a camera at near infrared wavelengths that can map the surface features of Titan according to reflectivity. The only regions hidden from the telescope's view are Titan's polar regions. The Cassini mission, comprising of a Saturn orbiter spacecraft and a Huygen probe is intended to address some of the uncertainties of the thick layer. The Huygens probe will be deployed, making a 2.25 hour decent down to the surface of Titan, profiling haze properties with altitude as well as a small portion of surface imaging. Cassini will then orbit Saturn for 3.5 years, resulting in approximately 43 flybys of Titan.

Due to budget limitations, future explorations of the outer planets are being constrained based on highest levels of priority with respect to science. In order to allow for the maximum gain in obtaining crucial science on a Titan mission in a cost efficient manner, the approach of utilizing an in situ oriented mission has been proposed, where direct communication with Earth is provided via an "aerobot", a relatively low Titan orbiting craft. Of significance, and addressed in our study, is the enabling technology for location awareness of this aerobot (blimp) and for other forms of passive and propelled aerial exploration vehicles. Although some level of navigation can be performed utilizing the direct long haul communication link with Earth, the potential wind speeds (speeds of up to 100 m/s at altitudes of ~200km) on Titan suggest a more real-time approach to navigation. Although data retrieval is not delay critical, navigation control may be required for an atmosphere with speeds of up to 100 m/s resulting in considerable uncertainties of relative positioning. Leveraging the high altitude air speeds while using a closed loop control of an aerobot via a direct long haul link to Earth involves roundtrip delays at best of ~2 hours, equating to control variations of up to 720 km. The low cost associated with a balloon and aerobot, or the programmatic appeal of the airship, helicopter, and tilt rotor approaches have made for a suite of potential exploration vehicles that demand accurate navigation capabilities to accomplish the science objectives.

2. ARCHITECTURE

There are numerous variations in potential in-situ navigation architectures and methods by which they may be deployed. However, all of the architectures of interest are composed of the following fundamental properties and capabilities:

1) In-situ coverage areas large enough such that they can be easily located by the in-situ vehicle when guided by long-haul course navigation.
2) A network of beacons for each location of scientific interest. A minimum of three is required for position estimation in three dimensions (for a single sample estimate, else two beacons could be sufficient with multiple estimates). Note that in the general case four nodes are required for high precision 3-D position estimation (as is the case in the global positioning system); however, location ambiguity can be removed by altimeter and other instruments that exist on the aerobot.
3) Individual beacons, or a subset of beacons, should be uniquely identifiable; this allows the aerobot to identify its unique location.
4) The aerobot must have memory of a) the unique beacons, b) the science locations associated with the beacons, and c) course estimates for the absolute global position of the network of beacons. These form the primary components of the navigation map.

The architectures have the following fundamental components:

1) Radio-frequency beacons
    a. Active or passive
2) Transmission technology
    a. Transceivers
    b. Antennas/reflectors
3) Navigation map
    a. Database of past location estimates
    b. Navigation algorithms

These primary components of a notional system are depicted in Figure 1. The course location estimates are obtained by the long-haul navigation link during deployment and when navigating between the networks of beacons. The fine location estimates may be obtained via in-situ communication with the networks of beacons. The storage of location information for all beacons, past location estimates and updates of real-time location estimation are accomplished by the navigation map. This navigation map contains algorithms for synthesizing course and fine location estimates, historical and real-time, and determining the current map for the aerial vehicle.

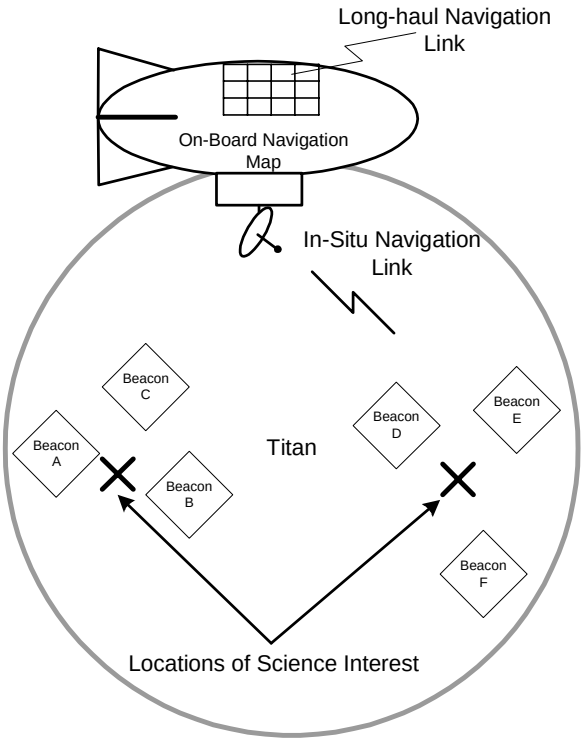

Figure 1- Navigation System

Note that during beacon deployment, the aerobot must estimate its location from the science target and store this location. In certain instances the beacon may be deployed in the same location as the science location, in others various instruments (i.e. altimeters, image processing) may be used to estimate the location of deployment relative to the science location. This location information is also integrated into the navigation map.

Ideally, when such architectures are developed in a systems engineering framework they should be developed to meet specific performance and resource requirements. Given the large number of variables in such an architecture, inherent risk and uncertainty in deploying engineering systems in an extra-terrestrial environment, and the early stages of development in which this development lies, we consider this to be a research problem. As such there are few fixed requirements presented here. However, we do present a high-level framework from which design choices, that are frequently mutually exclusive and competing, have been and continue to be derived. Again, one of our primary motivations is to reduce system cost and given the potential cost benefit of passive beacons, we focus on feasibility and tradeoffs with regard to coverage area and the type of beacon (active or passive) as shown below.

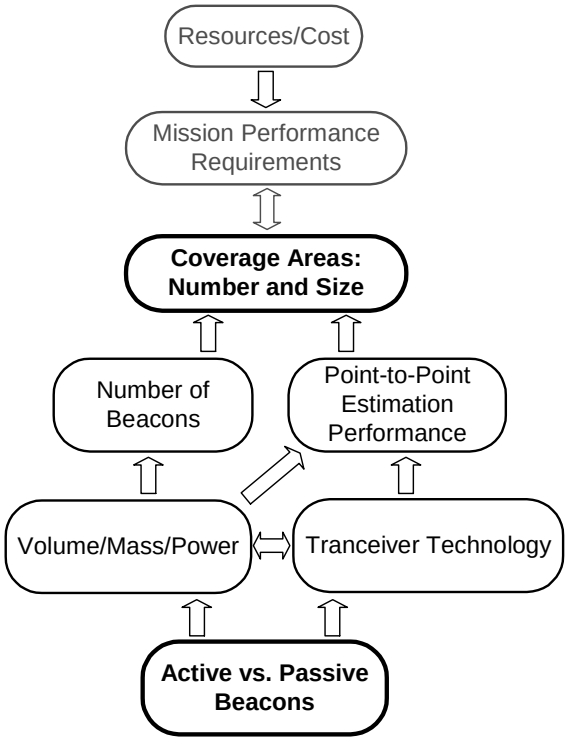

Figure 2- In-situ navigation tradestudy framework

It should be noted that the model represented above of the relationships between the major design parameters and subsystems is not unique. This model provides a well suited dual bottom-up/top-down perspective for determining the feasibility of the architecture with emphasis on coverage area and the type of beacon both of which have a large impact on cost (especially given the expense of nuclear power sources). While course approximations of the characteristics and performance of the subsystems above are utilized, the detailed performance of the various subsystems is not necessary to illustrate feasibility of the novel methods employing networks of passive beacons and their associated coverage areas. In addition such analysis, for example detailed transceiver or radar performance as a

function of signal-to-noise ratio, can be performed using conventional analysis and engineering design methods and will not be discussed here.

From the model depicted in Figure 2 we discuss two significant variations. One based on passive beacons, and one based on beacons with active power sources. Depending on the choice of active or passive beacons the architecture may employ a variety of existing and to-be-developed technologies derived from the areas of radar and wireless communications systems for performing point-to-point location determination and ranging estimation. We now proceed to discuss these two types of beacons.

3. ACTIVE VERSUS PASSIVE BEACONS

The passive radio frequency beacon (RF) is based in part on the mature technology of radio frequency identifying tags. RF-reflectors in conjunction with fundamental principles of radar, specifically radar cross-section of the beacons and the radar ambiguity function. The radar cross-section of the beacons is used in determining reflected beacon power; and is a necessary parameter in determining the link budget for the passive ranging system. The power density at the location of the reflector is:

$$S_{reflector} = \frac{P \times G}{4\pi \times R^2}$$

Where P is the transmit power, G is the gain of the transmit antenna, and R is the distance from transmitter to reflector. The passive beacon reflects power that is proportional to the power density S:

$$P_{reflected} = \sigma \times S$$

The radar cross section σ is a measure of the passive reflector's ability to reflect electromagnetic waves. The radar cross section depends on many parameters: size, shape, material, surface structure, background, wavelength, and polarization [7,8]. The power density that returns to the antenna of the ranging transceiver is:

$$S_{\mathrm{Re}ceive} = \frac{P \times G \times \sigma}{(4\pi)^2 \times R^4}$$

The reception power at the transceiver antenna on the aerial vehicle (refer to Figure 1) is:

$$P_{\mathrm{Re}ceive} = \frac{P \times G^2 \times \lambda^2 \times \sigma}{(4\pi)^3 \times R^4}$$

Where λ is the wavelength of the carrier frequency. The radar cross section of the dipole reflector is highly dependent on the properties of the surface on which it is placed, hence an accurate estimate of actual radar cross section is difficult to obtain; we have used standard academic models in the ranging link budget analysis presented here. The corner cube passive beacon was not considered primarily due to the difficulties likely to arise with deployment as well as the volume of these devices; although their use should be reconsidered if the gain of dipole reflectors cannot meet future ranging link budgets. The gain of the corner cube reflector is proportional to the square of its size; the gain of the simple dipole reflector is linearly proportional to its size. Knowledge of the radar cross-section and ambiguity function is necessary to determine the link budget (including estimation performance) of the in-situ navigation link and in turn the required size of the beacons, and the total number of beacons that may be sent and deployed in-situ to achieve the required coverage area. Estimates of these latter parameters are necessary to determine feasibility of the passive beacon approach. Preliminary link budgets, and size estimates of dipole beacons, are given in the link budget in Table 1 where the beacons are assumed to be isotropic scatterers [7,8].

Reflector Area	**Frequency**	**Transmit Power**	**Antenna Gain**	**Range**	**Received Power**
400 cm^2	2 Ghz	20 watts	20 dB	1 Km	-87 dBm
400 cm^2	2 Ghz	20 watts	20 dB	500 m	-75 dBm
400 cm^2	2 Ghz	5 watts	6 dB	100 m	-81 dBm
200 cm^2	4 Ghz	20 watts	20 dB	1 Km	-93 dBm
100 cm^2	4 Ghz	20 watts	20 dB	500 m	-81 dBm
100 cm^2	4 Ghz	5 watts	10 dB	100 m	-79 dBm

Table 1. Link Budget Assuming Passive Reflectors

Table one illustrates the feasibility of the passive beacons. Note that a range between transmitter and passive beacon of hundreds of meters or more is possible with antennas and reflector sizes that are realizable while still maintaining an acceptable reflected input power level at the transceiver input (based on the current state-of-the art low-noise amplifiers). Also note that antenna and reflector sizes are dependant on transmission frequencies; frequencies were chosen for the link analysis to keep these sizes relatively small in size.

While the beacons themselves are passive, the ranging transceiver must of course be active. The transceiver-bearing aerobot can determine its precise (relative) position in a network of beacons by transmitting a ranging code and receiving and processing the RF reflection (there are other methods as well [2]). The appropriate location estimation techniques, their statistical properties (variance for instance) for given power levels, and integration times may be readily determined [2].

The passive beacons may be constructed from a variety of materials and with varying physical configurations and are likely have relatively small mass relative to an active beacons, facilitating the launch and deployment of a much larger number of beacons. In addition the operation life of a passive beacon is potentially many years or decades depending on the in-situ environment. A key characteristic of the beacon, passive or active, is that it be uniquely identifiable by the in-situ aerobot. This can be accomplished in a variety of ways. One method is to design each passive beacon with a unique antenna patter that can be detected by the transceiver on the aerobot [7,8]. Another method utilizes identical beacons, but beacons are deployed two or more at a time in unique configurations such that

unique radio frequency reflections can be identified by the transceiver on the aerobot.

Current battery and solar cell technologies are not realizable sources of power for beacons on Titan. Given current technology only nuclear powered beacons would be possible. In future this may change. Deep space missions have a strong need for compact, high power density, reliable and long life electrical power generation and storage under extreme temperature conditions. Conventional power generating devices become inefficient at very low temperatures and rechargeable energy storage devices cannot be operated thereby limiting mission duration. At elevated temperatures thin film interdiffusion destroy electronic devices used for generating and storing power. Solar power generation strongly depends upon the light intensity, which falls rapidly in deep interplanetary missions (beyond 5 a.u.), and in planetary missions in the sun shadow or in dusty environments.

Radioisotope thermoelectric generators (RTGs) have been successfully used for a number of deep space missions. However, their energy conversion efficiency and specific power characteristics are low, and this technology has been limited to relatively large systems (more than 100W). Innovative technologies that will function reliably over a long duration mission, ten years or more, in harsh environments (temperature and atmosphere for example) must be developed to enable the success of future space missions such as the proposed mission to Titan. It is also expected that such micro power sources could have a wide range of terrestrial applications, in particular when the limited lifetime and environmental limitations of batteries are key factors. Mission insertion and benefits: This technology is expected to be ready for consideration within 4 to 5 years [4,5].

Advanced solid-state thermoelectric or alpha-voltaic microdevices combined with radioisotope sources and energy storage devices such as capacitors are ideally suited for these applications. JPL is pursuing the development of innovative thermoelectric microdevices using integrated-circuit type fabrication processes, electrochemical deposition techniques and high thermal conductivity substrate materials. An even higher degree of miniaturization and high specific power values (mW/mm^3) can be obtained when considering the potential use of radioisotope for Europa (ice transceivers) or Mars [4,5].

Assuming such technologies mature an active beacon technology might be developed and deployed by the aerobot. The point-to-point estimation performance of the navigation system (Figure 1) utilizing powered transmitters/beacons can be readily estimated using appropriate well known system analysis methods (appropriate antenna gains, PN-ranging or ultra-wideband (pulse-radar) systems technology, etc.) [2,7,8].

4. COVERAGE PROBLEM

In this section, we examine beacon density and spatial placement based on type of real-time science observed (refer to Figure 2). We extend the concept of two types of localization in [3] by refining the cases to three types of science localization techniques; non-overlapping proximity (general vicinity/directional information), overlapping proximity (intersection through proximity localization) and multilateration (triangulation techniques). The objective in non-overlapping proximity is to utilize the beacon ranging to recognize the general vicinity of the aerobot, whereby direction information is gleaned such that other science gathering techniques can then obtain more accurate localization. In overlapping proximity and multilateration, the objective is to resolve the specific location of the aerobot within some mean error. As we increase the density of the beacons, mean localization error decreases, where there is diminishing return due to interference for densities greater than 0.01 beacons per sq m (~7 beacons per nominal radio coverage area for RF radial power range 15 meters) [3]. Due to cost considerations (limited number of beacons), we aim to obtain maximal coverage area with the minimal number of beacons for proximity localization and multilateration.

Non-overlapping Proximity

We can extract coverage area simply by calculating the spatial coverage of a beacon. Assuming omni directional beacons, and that none of the radial coverage of a beacon is overlapping (i.e. only one beacon is heard at any time), we have the area πR^2 where R is the radius of the beacon coverage. Suppose we previously placed beacons around a point of science. We can then calculate the likelihood of detecting at least one beacon in a single pass of the aerobot's flight path, given some course grain error. As depicted in Figure 3, using course grain navigation from Earth provides the sample location of aerobot with some error vector $\boldsymbol{d_E}$. Thus, the probability of the aerobot detecting at least one beacon is

$$p(n, d_E) = \frac{n\pi R^2}{(2d_E)(2R)} = \frac{n\pi R}{4d_E},$$

where $\boldsymbol{n}$ is the number of non-overlapping beacons, R is the radial coverage of a beacon, and $\boldsymbol{d_E}$ is the acceptable worst-case error due to course grain location estimate and environmental conditions.

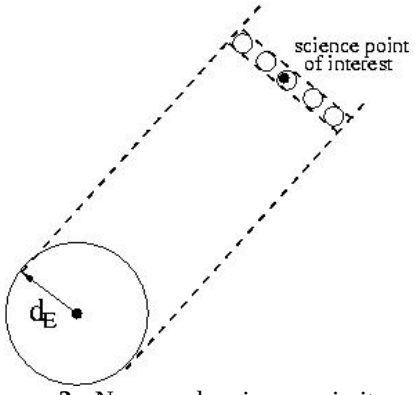

Figure 3 - Non-overlapping proximity case

Overlapping proximity/Multilateration

For the case of localization where relative 3 space coordinates are desired, we can develop an algorithm using overlapping proximity, multilateration, or possibly both where overlapping proximity reduces the possible coordinates to an area (i.e. equivalent to some coordinates with some large localization error) then precise triangulation techniques further reduce the localization error.

We must first consider the amount of overlapping relative to the amount of non-overlapping nodes. In the specific 2-ode case, as depicted in Figure 4 we see that the amount of overlap ranges from 0 to 2π.

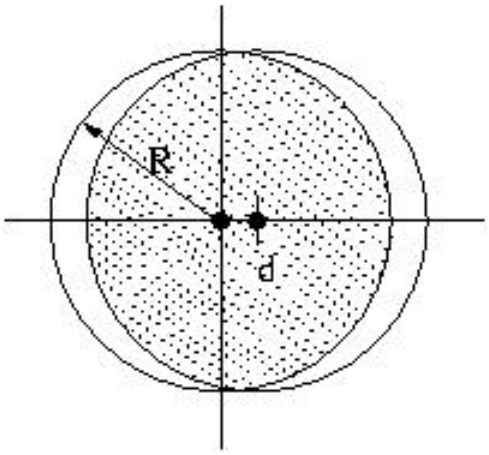

Figure 4-Amount of overlap for 2 nodes

We now formally identify the amount of overlap region (shaded in Figure 4 and the amount of at least one node regions for the two node case (both shaded and unshaded regions).

Using a single quadrant as in Figure 5, we can express the overlapping area and at least one node within region area in terms of areas α_1, α_2, and α_3.

The total area of overlap, $A_{2(d)}$ is

$$A_{2(d)} = 2(2\alpha_3 - \alpha_2) \qquad (1)$$

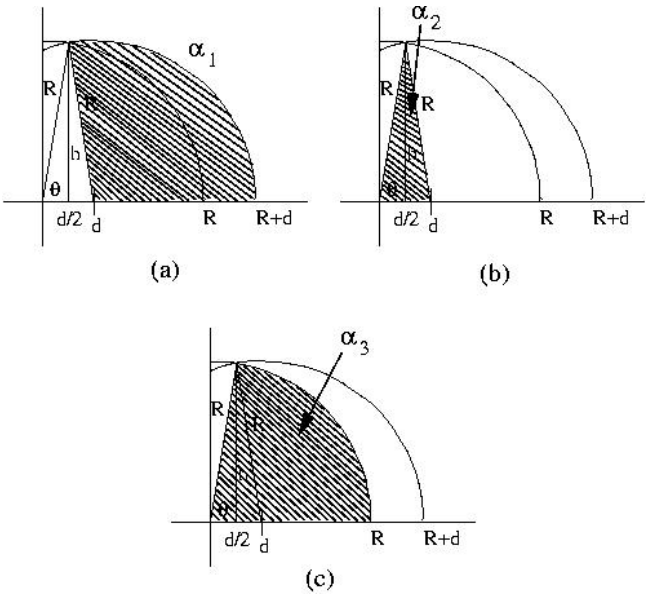

Figure 5 - Overlapping versus non-overlapping regions in a single quadrant 2-node case

The total area covered by at least one node is

$$A_{1+2(d)} = 4\alpha_1 + 2\alpha_2 \qquad (2)$$

Using Figure 5 (a), (b), and (c), we now solve for θ, α_1, α_2, and α_3.

Recognize that the angle of the arc in the first quadrant generated by the intersection of the circle centered at the origin and the circle centered at (d,0) is

$$\theta = \cos^{-1}\frac{d}{2R} \qquad (3)$$

Recognize that the shaded area in Figure 3(a) is

$$\alpha_1 = \int_{r=0}^{R}\int_{0}^{\frac{\pi}{2}+\frac{\pi}{2}-\theta} r\,dr\,d\Theta$$
$$= \frac{R^2}{2}(\pi - \theta). \qquad (4)$$

where θ spans 0 to π/2. Equivalently, this is d spanning between 0 and 2R.

Recognize that the shaded area in Figure 5(b) is

$$\alpha_2 = \frac{1}{2}dh$$
$$= \frac{Rd\sqrt{1-\left(\frac{d}{2R}\right)^2}}{2} \qquad (5)$$

Recognize that the shaded area in Figure 5(c) is

$$\alpha_3 = \int_{r=0}^{r=R}\int_{0}^{\theta} r\,dr\,d\Theta = \frac{R^2}{2}\theta \qquad (6)$$

Using (1), (3), (5) and (6), we have

$$A_{2(d)} = 2(2\alpha_3 - \alpha_2) = 2\left(2\frac{R^2}{2}\theta - \frac{Rd\sqrt{1-\left(\frac{d}{2R}\right)^2}}{2}\right)$$

$$= 2R^2\cos^{-1}\frac{d}{2R} - \frac{Rd\sqrt{1-\left(\frac{d}{2R}\right)^2}}{2}$$

$$= R\left(2R\cos^{-1}\frac{d}{2R} - d\sqrt{1-\left(\frac{d}{2R}\right)^2}\right) \qquad (7)$$

Recognize that at d=2R, we have $A_{2(d)} = 0$ as expected (i.e. the two coverage areas have zero overlap). At the other extreme, when d=0 we have πR^2, as expected, since both nodes reside on top of each other. Clearly, maximum overlap occurs when both nodes reside on top of each other. However, the ability to accurately perform a single 2-D relative location estimate and a 3-D relative location estimate reduces as the nodes are placed closer to each other.

Now for the total coverage (with at least one node), using (2)-(8), we have

$$A_{1+2(d)} = 4\alpha_1 + 2\alpha_2 = 4\frac{R^2(\pi-\theta)}{2} + 2\frac{Rd\sqrt{1-\left(\frac{d}{2R}\right)^2}}{2}$$

$$= 2R^2(\pi-\theta) + Rd\sqrt{1-\left(\frac{d}{2R}\right)^2}$$

$$= 2R^2\left(\pi - \cos^{-1}\frac{d}{2R}\right) + Rd\sqrt{1-\left(\frac{d}{2R}\right)^2} \qquad (8)$$

Recognize that as d inceases (from 0 to 2R), the first term in (8) increases to $2\pi R^2$ and the second term goes to 0. As d decreases to 0, the first term tends to πR^2 while the second term goes to 0.

Due to symmetry, we now consider the cases where the nodes are placed at a distance R apart from each other. Under this specific constraint, we examine various cases of either employing a single sample of ranging (from multiple beacons) or multiple samples of ranging from multiple beacons (from multiple locations).

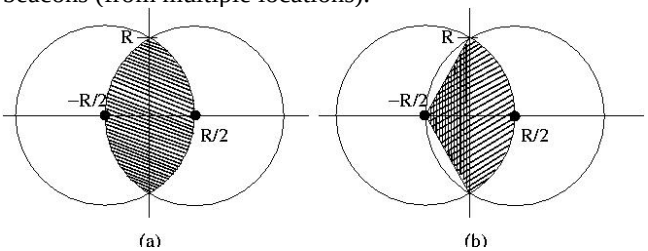

Figure 6 - Overlapping region 2 node cases

Collecting at least two samples from two beacons such as in the case where an aerobot obtains a ranging estimate from both beacons, moves and then obtains a second sample, motivates examination for the overlapping coverage area problem. Thus, for the two beacon case as shown if Figure 6(a), we have

$$A_2 = \frac{2\pi R^2}{3} - \frac{\sqrt{3}R^2}{2} \qquad (9)$$

Formally, we obtain (9) from Figure 6(a) and (b) by eliminating the triangular hashed part of the arc in (b) from the arc and doubling the result.

$$A_2 = 2\left[\left(\frac{R^2}{2}\int_{-\pi/3}^{\pi/3} d\theta\right) - \frac{1}{2}\left(\sqrt{3}R\right)\left(\frac{R}{2}\right)\right]$$

$$= 2\left[R^2\frac{\pi}{3} - \frac{\sqrt{3}R^2}{4}\right]$$

$$= \frac{2\pi R^2}{3} - \frac{\sqrt{3}R^2}{2}.$$

For the 3 beacon case, overlapping of at least 2 beacons, can be obtained by summing up the region of two overlapping coverage areas and the three overlapping coverage areas. Equivalently, the 3 beacon case with at least 2 beacon overlapping regions could be solved by summing the two node area case using (9) and two smaller two overlapping regions as in Figure 7.

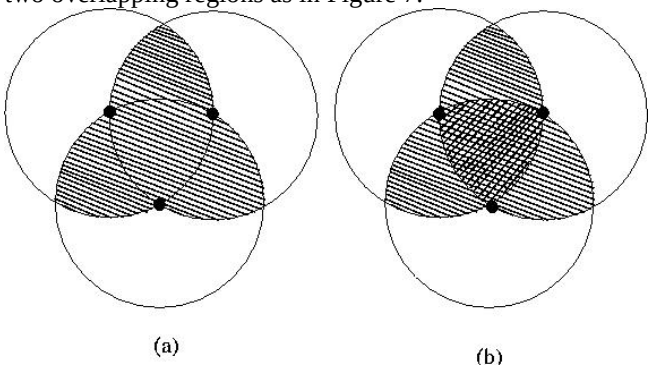

Figure 7 - 3 node case

Thus, we have for at least 2-nodes of overlap,

$$A_2(3) = A_2 + 2\left[\frac{A_2}{2} - \left[\left(\frac{R^2}{2}\int_{-\pi/6}^{\pi/6} d\theta\right) - \frac{R}{2}\frac{\sqrt{3}R}{2}\right]\right]$$
$$= A_2 + A_2 - 2\left(\frac{\pi R^2}{6} - \frac{\sqrt{3}R^2}{4}\right)$$
$$= 2A_2 - \frac{\pi R^2}{3} + \frac{\sqrt{3}R^2}{2}$$
$$= 2\left(\frac{2\pi R^2}{3} - \frac{\sqrt{3}R^2}{2}\right) - \frac{\pi R^2}{3} + \frac{\sqrt{3}R^2}{2}$$
$$= \frac{4\pi R^2}{3} - \sqrt{3}R^2 - \frac{\pi R^2}{3} + \frac{\sqrt{3}R^2}{2}$$
$$= \pi R^2 - \frac{\sqrt{3}R^2}{2}. \qquad (10)$$

Similarly, for the case of 3 beacons with exactly a three overlapping beacon coverage area as in Figure 7(b), we have

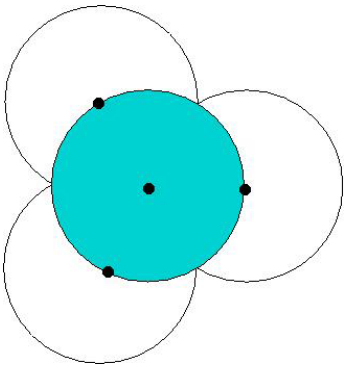

Figure 8 - 4 nodes with at least 2 nodes overlapping

For the case of 4 beacons, as observed in Figure 8, if at least 2 beacons overlap, the straight forward result is

$$A_2(4) = \pi R^2. \qquad (4)$$

As depicted in Figure 6 and 8, we can extend this concept of minimal coverage area and calculate the number of nodes required for at least 2 beacon coverage as the minimal case; we call this the 2-cover.

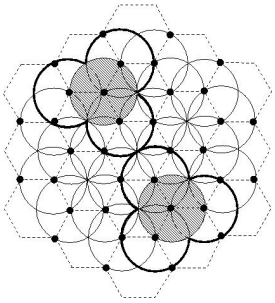

Figure 9 - Honeycomb dispersal of beacons to povide 2-cover

We observe from Figure 8 and 9 that careful dispersal in groups of 4 nodes provide coverage areas equivalent to the area of a circle of radius ***R***.

We now consider the inverse, or rather, given the number of beacons, we can obtain the 2-cover area in terms of the RF radial coverage ***R*** of a beacon. Using (4), we can equivalently express the minimum obtainable 2-cover area as

$$A_2(n) \geq \pi R^2 \left\lfloor \frac{n}{4} \right\rfloor \qquad (5)$$

Figure 10 depicts the cases when ***n*** is divisible by 4. In addition, Figure 10 provides an example case for a possible sample radius using the passive beacon approach.

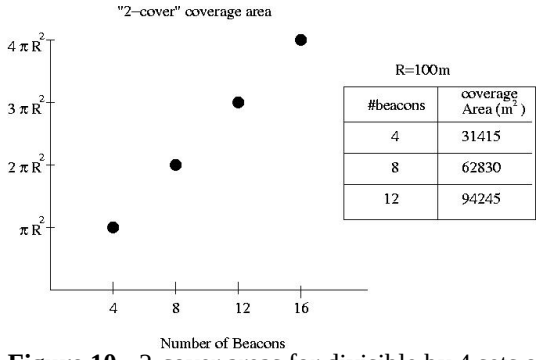

Figure 10 - 2-cover areas for divisible by 4 sets of nodes

Recall the 3 node case. Recognize that it is possible to place the nodes such that there is only 2-cover area. Specifically, an upper bound on the 3-node 2-cover case is twice A_2. Extending this concept for the n node case, we have

$$A_2(n) = \pi R^2 \left\lfloor \frac{n}{4} \right\rfloor + n_{\text{mod}\,4} A_2$$
$$= \pi R^2 \left\lfloor \frac{n}{4} \right\rfloor + n_{\text{mod}\,4} \left(\frac{(4\pi - 3\sqrt{3})R^2}{6}\right)$$

where mod is the modulo of the number. Thus, for n that is not divisible by 4, we increase by a factor of n modulo 4 times .39 of πR^2. Specifically, we have

$$A_2(n) \approx \left(\left\lfloor \frac{n}{4} \right\rfloor + 0.39 n_{\text{mod}\,4}\right)\pi R^2.$$

5. CONCLUDING REMARLKS

In this paper, we presented a study and procedures for developing architectures for in-situ location determination on Titan. We designed such an architecture and presented its primary components and characteristics. We presented the novel use of networks of passive beacons for obtaining in-situ location estimates and demonstrated their feasibility and approximated operational ranges. Coverage areas as a function of operational range were derived. From this

realistic coverage area can be obtained for an architecture utilizing a network of beacons based on point-to-point performance analysis and the number of beacons in the network. The current state-of-the art in power generation for active beacons on Titan was discussed; RTGs are currently the only way to power such beacons in that environment. Finally, science oriented coverage area requirements for a topologically efficient placement of the beacons to allow for high precision location determination was developed.

REFERENCES

[1] Ralph D. Lorenz, "Post-Cassini Exploration of Titan: Science Rationale and Mission Concepts", JBIS, Vol. 53, pp. 218-234, 2000.
[2] M. K. Simon, J. Omura, R. A. Scholtz, B. K. Levitt, *Spread Spectrum Communications Handbook*, Mcgraw-Hill, New York, 1994.
[3] Nirupama Bulusu, John Heidemann, Deborah Estrin, "Adaptive Beacon Placement", *Proceeding of the 21st International Conference on Distributed Computing Systems (ICDCS 21)*, Phoenix, Arizona, April 2001.
[4] J. P. Fleurial, J. Patel, G.J. Snyder, C. K. Huang, R. Averback, C. Hill, G. Chen, Jet Propulsion Laboratory "Solid-state power generating microdevices for distributed space system architectures," innovative approaches to outer exploration 2001-2002".
[5] M. A. Ryan and J.-P. Fleurial, "Where There Is Heat, There Is a Way: Thermal to Electric Power Conversion Using Thermoelectric Micro-converters," The Electrochemical Society *Interface* • Summer 2002
[6] K. Finkenzeller, RFID Handbook, John Wiley and Son, LTD, Chichester, 1999.
[7] Merrill Skolnik, Introduction to Radar Systems, 3rd edition, McGraw-Hill, 2001
[8] Merrill Skolnik, Radar Handbook, 2nd edition, McGraw-Hill Professional, 1990

Andrew Gray *received the PhD in electrical engineering from the University of Southern California in May of 2000 and the MS in electrical engineering from the Johns Hopkins University in May of 1997. He has been with the Jet Propulsion Laboratory, Communication Systems and Research Section since 1998. Previously he was a contractor with NASA's Goddard Space Flight Center, Microelectronics and Signal Processing Branch. He is the primary architect of NASA's 600 Mbps all digital receiver and the next generation 2.4 Gbps QPSK/16-QAM all digital receiver for bandwidth efficient satellite communications. He has over thirty publications and patents in the areas of signal processing, communications, and VLSI architectures for communications systems. His research interests include wireless communications, parallel and multirate digital processing for high rate bandwidth efficient wireless communications systems, network communications, and intelligent systems. Dr. Gray also serves on the affiliate graduate faculty of the University of Washington, Seattle.*

Clayton Okino *received a BS in Electrical Engineering at Oregon State University in 1989, a MS in Electrical Engineering at Santa Clara University in 1993, and a Ph.D. in Electrical and Computer Engineering from the University of California, San Diego in 1998. After receiving his Ph.D., Dr. Okino accepted a position as an assistant professor in Thayer School of Engineering at Dartmouth College, where he pursued research in communication and wireless networks, emphasizing on performance and security. In 2001, Dr. Okino accepted a position as a Senior Member of the Technical Staff in the Digital Signal Processing group at Jet Propulsion Laboratory where his current research is in wireless network routing and access algorithms, reconfigurable sensors, wireless QoS and location based processing techniques.*

Esther Jennings *received her BS in Computer Science at the University of California, Riverside, in 1982. In 1991, she received her MS in Computer Science from Lund University, Sweden. She received a Ph.D. in Computer Science from the Luleå University of Technology, Sweden, in 1997. From 1997-1999, she was a postdoctoral fellow at the IndustrialEngineering Department at Technion, Israel Institute of Technology. From 1999-2001, she has been an assistant professor at the Computer Science Department of California State Polytechnic University, Pomona. She is currently a member of technical staff at the Jet Propulsion Laboratory. Her research interests are in distributed graph algorithms, reliable multicast protocols, scheduling algorithms in optical switches and energy-efficient algorithms for wireless networks.*